Inorg. Chem. **2008**, *47*, 578–583

Ferrocenoyl Pyridine Arene Ruthenium Complexes with Anticancer Properties: Synthesis, Structure, Electrochemistry, and Cytotoxicity

Mathieu Auzias,[†] Bruno Therrien,[†] Georg SUss-Fink,*[,†] Petr Štěpnička,[‡] Wee Han Ang,[§] and Paul J. Dyson[§]

Institut de Chimie, Université de Neuchâtel, Case postale 158, CH-2009 Neuchâtel, Switzerland, Charles University, Faculty of Science, Department of Inorganic Chemistry, Hlavova 2030, CZ-12840 Prague 2, Czech Republic, and Institut des Sciences et Ingénierie Chimiques, Ecole Polytechnique Fédérale de Lausanne (EPFL), CH-1015, Lausanne, Switzerland

Received September 21, 2007

Organometallic ruthenium(II) complexes of general formula [Ru(η^6-arene)Cl_2(NC_5H_4OOC–$C_5H_4FeC_5H_5$)], where arene = C_6H_6 (**1**), C_6H_5Me (**2**), *p*-^{i}PrC_6H_4Me (**3**), and C_6Me_6 (**4**), and of general formula [Ru(η^6-arene)Cl_2]$_2$(NC_5H_4OOC–$C_5H_4FeC_5H_4$–$COOC_5H_4N$), where arene = *p*-^{i}PrC_6H_4Me (**5**) and C_6Me_6 (**6**), have been synthesized and characterized, the molecular structures of these complexes being confirmed by single-crystal X-ray structure analysis of complex **4** as a representative example. The redox properties and in vitro anticancer activities of complexes **1**–**6** have been studied. All the compounds are moderately cytotoxic toward the A2780 and A2780cisR (cisplatin-resistant) human ovarian carcinoma cell lines. The diruthenium arene complexes **5** and **6** are about twice as active as their mononuclear analogues **3** and **4**. Cyclic voltammetry revealed a good correlation of the Ru^{II}/Ru^{III} redox potentials of **1**–**4** and the number of alkyl substituents in the arene ligand.

Introduction

The search for metal-based antitumor drugs results from the discovery by Rosenberg in 1965 that cisplatin could effectively inhibit tumor growth,[1] and subsequently cisplatin has become the most widely used anticancer drug in the world.[2] Rosenberg's discovery stimulated the quest for other platinum-based drugs since, although cisplatin is extensively used in cancer therapy, its toxicity is high, leading to side effects which limit administered dose,[3] and some tumors are resistant to cisplatin.[4] Apart from the development of other platinum drugs, other metal-based anticancer agents have been developed which appear to exhibit fewer side effects. Prominent examples include metallocenes, such as titanocene dichloride,[5−7] and ferrocene derivatives of tamoxifen, e.g., Ferrocifens (see Figure 1).[8] Very recently, two ruthenium(III) complexes have also successfully completed phase I clinical trials, namely, NAMI-A[9−11] and KP1019.[12−13]

* To whom correspondence should be addressed. E-mail: georg.suess-fink@unine.ch.
[†] Université de Neuchâtel.
[‡] Charles University.
[§] Institut des Sciences et Ingénierie Chimiques.

(1) Rosenberg, B.; VanCamp, L.; Trosko, J. E.; Mansour, V. H. *Nature* **1969**, *222*, 385−386.
(2) (a) Reedijk, J. *Chem. Commun.* **1996**, *7*, 801−806. (b) Wong, E.; Giandomenico, C. M. *Chem. Rev.* **1999**, *99*, 2451−2461 and references cited therein. (c) Boulikas, T.; Vougiouka, M. *Oncol. Rep.* **2003**, *10*, 1663−1682.
(3) (a) Chu, G. *J. Biol. Chem.* **1994**, *269*, 787−790. (b) Fuertes, M. A.; Alonso, C.; Perez, J. M. *Chem. Rev.* **2003**, *103*, 645−662. (c) Agarwal, R.; Kaye, S. B. *Nat. Rev. Cancer* **2003**, *3*, 502−516.
(4) Wang, D.; Lippard, S. J. *Nat. Rev. Drug Discov.* **2005**, *4*, 307−320.
(5) Köpf-Maier, P.; Köpf, H. *Chem. Rev.* **1987**, *87*, 1137−1152.
(6) Kröger, N.; Kleeberg, U. R.; Mross, K.; Edler, L.; Sass, G.; Hossfeld, D. K. *Onkologie* **2000**, *23*, 60−62.
(7) Carso, F.; Rossi, M. *Mini-Rev. Med. Chem.* **2004**, *4*, 49−60.
(8) Top, S.; Vessières, A.; Cabestaing, C.; Laios, I.; Leclercq, G.; Provot, C.; Jaouen, G. *J. Organomet. Chem.* **2001**, *637*−*639*, 500−506.
(9) Sava, G.; Bergamo, A. *Int. J. Oncol.* **2000**, *17*, 353−365.
(10) Rademaker-Lakhai, J. M.; Van den Bongard, D.; Pluim, D.; Beijnen, J. H.; Schellens, J. H. *Clin. Cancer Res.* **2004**, *10*, 3717−3727.
(11) (a) Sava, G.; Gagliardi, R.; Bergamo, A.; Alessio, E.; Mestroni, G. *Anticancer Res.* **1999**, *19*, 969−972. (b) Bergamo, A.; Gava, B.; Alessio, E.; Mestroni, G.; Serli, B.; Cocchieto, M.; Zorzet, S.; Sava, G. *Int. J. Oncol.* **2002**, *21*, 1331−1338. (c) Groessl, M.; Reisner, E.; Hartinger, C. G.; Eichinger, R.; Semenova, O.; Timerbaev, A. R.; Jakupec, M. A.; Arion, V. B.; Keppler, B. K. *J. Med. Chem.* **2007**, *50*, 2185−2193.
(12) (a) Hartinger, C. G.; Zorbas-Seifried, S.; Jakupec, M. A.; Kynast, B.; Zorbas, H.; Keppler, B. K. *J. Inorg. Biochem.* **2006**, *100*, 894−904. (b) Kapitza, S.; Pongratz, M.; Jakupec, M. A.; Heffeter, P.; Berger, W.; Lackinger, L.; Keppler, B. K.; Marian, B. *J. Cancer Res. Clin. Oncol.* **2005**, *131*, 101−110. (c) Keppler, B. K.; Henn, M.; Juhl, U. M.; Berger, M. R.; Niebl, R.; Wagner, F. E. *Prog. Clin. Biochem. Med.* **1989**, *10*, 41−69. (d) Pongratz, M.; Schluga, P.; Jakupec, M. A.; Arion, V. B.; Hartinger, C. G.; Allmaier, G.; Keppler, B. K. *J. Anal. At. Spectrom.* **2004**, *19*, 46−51.

10.1021/ic7018742 CCC: $40.75
Published on Web 12/18/2007

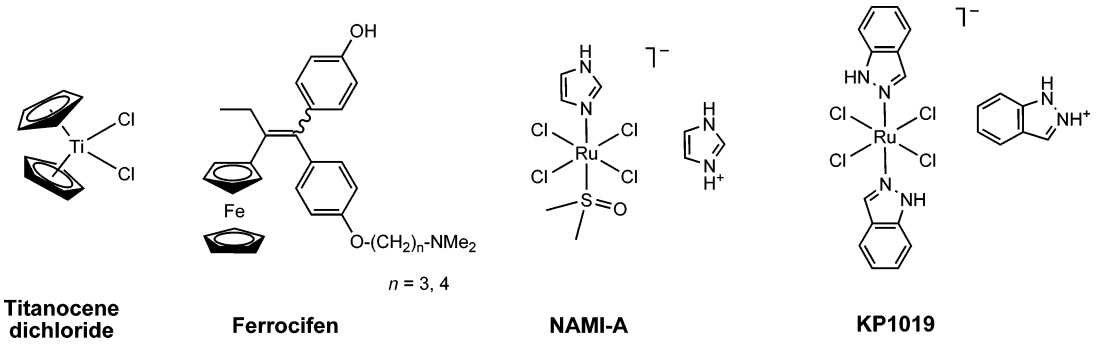

Figure 1. Molecular representations of non-platinum drugs evaluated for anticancer activity.

Scheme 1. Synthesis of Complexes **1**−**6**

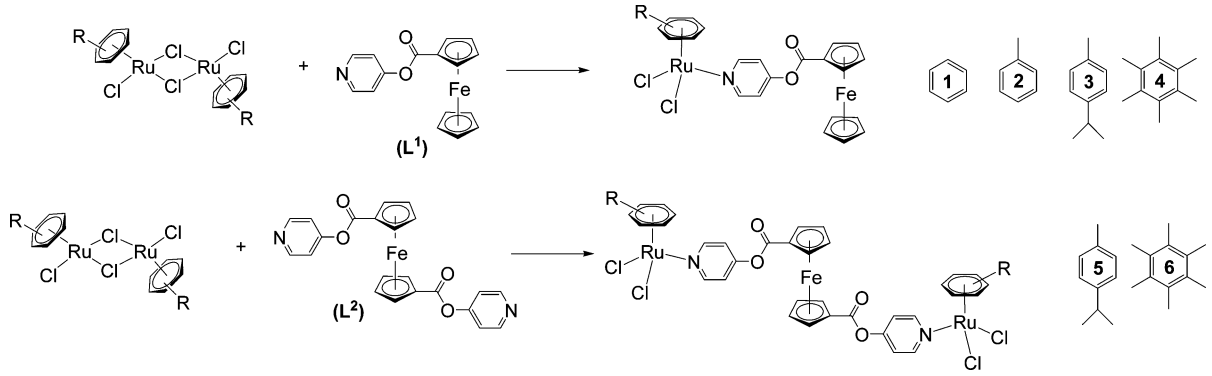

Iron- and ruthenium-based drugs appear to be good alternatives to platinum drugs, and considerable advances have been made on anticancer drugs based on these metals.[14−15] Some simple ferrocene compounds show excellent cytotoxicities in vitro and inhibit the development of tumors in vivo.[16] A more widespread approach pioneered by Jaouen is to append biologically active molecules to the ferrocenyl unit which increases the potency of the organic compound, possibly due to the combined action of the organic molecule with Fenton chemistry of the Fe center.[17] Ferrocene has also been linked to both platinum[18−19] and gold[20] centers in order to achieve synergistic effects between the two active metals. In general the iron compounds are well tolerated in vivo, and similarly, ruthenium compounds exhibit low general toxicity compared to their platinum counterparts, which is probably due to two main reasons. First, ruthenium compounds specifically accumulate in rapidly dividing cells, such as tumors, due to the ability of ruthenium to mimic iron in binding to transferrin,[12d] the protein which delivers iron to cells, and transferrin receptors are overexpressed in cancer cells.[21] Second, the majority of ruthenium drugs comprise ruthenium in the +3 oxidation state, and it has been proposed that in this oxidation state ruthenium is less active and reduced in vivo to more active ruthenium(II) complexes, a process favored in the hypoxic environment of a tumor.[21e,f] However, it should be noted that ruthenium(II) compounds also exhibit a low general toxicity, and since cancer cells can also become oxidizing at certain stages of their growth cycle, oxidation of the ruthenium cannot be excluded.[22]

Since arenes are known to stabilize ruthenium in its +2 oxidation state, the potential of Ru(II) arene complexes as anticancer agents and their associated aqueous chemistry is becoming increasingly investigated. The first complex evaluated of this kind was [Ru(η^6-benzene)Cl_2(metronidazole)], which had a higher activity compared to the antitumor drug metronidazole itself;[23] more recently [Ru(η^6-arene)(pta)Cl_2][24]

(13) Kreuser, E. D.; Keppler, B. K.; Berdel, W. E.; Piest, A.; Thiel, E. *Semin. Oncol.* **1992**, *19*, 73−81.
(14) (a) Pigeon, P.; Top, S.; Vessières, A.; Huché, M.; Hillard, E. A.; Salomon, E.; Jaouen, G. *J. Med. Chem.* **2005**, *48*, 2814−2821. (b) Vessières, A.; Top, S.; Beck, W.; Hillard, E.; Jaouen, G. *Dalton Trans.* **2006**, 529−541.
(15) Ang, W. H.; Dyson, P. J. *Eur. J. Inorg. Chem.* **2006**, 4003−4018.
(16) (a) Popova, L. V.; Babin, V. N.; Belousov, Y. A.; Nekrasov, Y. S.; Snegireva, A. E.; Borodina, N. P.; Shaposhnikova, G. M.; Bychenko, O. B.; Raevskii, P. M. *Appl. Organomet. Chem.* **1993**, *7*, 85−94. (b) Köpf-Maier, P.; Köpf, H.; Neuse, E. W. *J. Cancer Res. Clin.* **1984**, *108*, 336−340.
(17) Hillard, E.; Vessieres, A.; Le Bideau, F.; Plażuk, D.; Spera, D.; Huché, M.; Jaouen, G. *Chem. Med. Chem.* **2006**, *1*, 551−559 and references cited therein.
(18) Henderson, W.; Alley, S. R. *Inorg. Chim. Acta* **2001**, *322*, 106−112.
(19) Rosenfeld, A.; Blum, J.; Gibson, D.; Ramu, A. *Inorg. Chim. Acta* **1992**, *201*, 219−221.
(20) Viotte, M.; Gautheron, B.; Kubicki, M. M.; Nifant'ev, I. E.; Fricker, S. P. *Met.-Based Drugs* **1995**, *2*, 311−326.
(21) (a) Messori, L.; Gonzales Vilchez, F.; Vilaplana, R.; Piccioli, F.; Alessio, E.; Keppler, B. *Met.-Based Drugs* **2000**, *7*, 335−342. (b) Timerbaev, A. R.; Hartinger, C. G.; Aleksenko, S. S.; Keppler, B. K. *Chem. Rev.* **2006**, *106*, 2224−2248. (c) Hartinger, C. G.; Ang, W. H.; Casini, A.; Messori, L.; Keppler, B. K.; Dyson, P. J. *J. Anal. At. Spectrom.* **2007**, *22*, 960−967. (d) Polec-Pawlak, K.; Abramski, J. K.; Semenova, O.; Hartinger, C. G.; Timerbaev, A. R.; Keppler, B. K.; Jarosz, M. *Electrophoresis* **2006**, *27*, 1128−1135. (e) Clarke, M. J.; Bitler, S.; Rennert, D.; Buchbinder, M.; Kelman, A. D. *J. Inorg. Biochem.* **1980**, *12*, 79−87. (f) Schluga, P.; Hartinger, C. G.; Egger, A.; Reisner, E.; Galanski, M.; Jakupec, M. A.; Keppler, B. K. *Dalton Trans.* **2006**, *14*, 1796−1802.
(22) Dyson, P. J.; Sava, G. *Dalton Trans.* **2006**, 1929−1933.

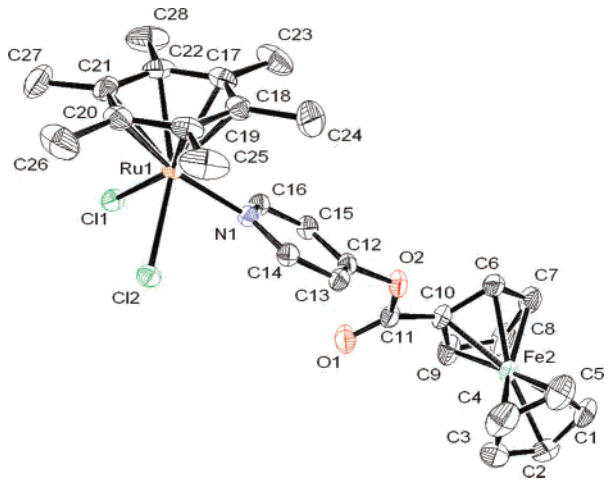

Figure 2. ORTEP representation of **4** at 50% probability level, hydrogen atoms, and the solvating chloroform molecules being omitted for clarity. Selected bond lengths (Å) and angles (deg): Ru(1)−Cl(1) 2.4219(5), Ru(1)−Cl(2) 2.4162(5), Ru(1)−N(1) 2.123(2), C(12)−O(2) 1.386(2), O(2)−C(11) 1.375(3), C(11)−O(1) 1.197(3), C(10)−C(11) 1.456(3); Cl(1)−Ru(1)−Cl(2) 88.00(2), N(1)−Ru(1)−Cl(1) 85.70(5), N(1)−Ru(1)−Cl(2) 84.97(5), C(12)−O(2)−C(11) 117.9(2), O(1)−C(11)−O(2) 122.4(2), O(1)−C(11)−C(10) 127.2(2).

(pta = 1,3,5-triaza-7-phosphatricyclo[3.3.1.1]decane), [Ru(η^6-arene)(YZ)(Cl)][PF_6][25] (YZ = chelating diamine), and the tri-[26] and tetranuclear[27] clusters such as [H_3Ru_3(η^6-C_6H_6)(η^6-C_6Me_6)$_2$O]$^+$ and [H_4Ru_4(η^6-C_6H_6)$_4$]$^{2+}$ have been studied in vitro for their activity.

However, to our knowledge, attempts to combine ruthenium and iron within the same molecule as putative anticancer agents have not been reported. In this paper we describe compounds of general formula [Ru(η^6-arene)Cl_2]$_n$-(L) bearing terminal (n = 1) or bridging (n = 2) ferrocene-modified pyridine ligands (L). The synthesis, characterization, and in vitro cytotoxic activity on A2780 and A2780cisR (human ovarian carcinoma) cell lines of this series of new ruthenium(II)−arene complexes are described as well as their electrochemical behavior.

Results and Discussion

Reaction of the dimers [Ru(η^6-arene)Cl_2]$_2$ (arene = benzene, toluene, *p*-cymene, or hexamethylbenzene)[28] in dichloromethane at room temperature or toluene under reflux with 2 equiv of the ferrocenoyl substituent ligand[29] (NC_5H_4-OOC−$C_5H_4FeC_5H_5$) **L**^{1} affords **1**−**4** or with 1 equiv of the dipyridyl ferrocene derivative ligand[30] ($NC_5H_4OOC-C_5H_4$-$FeC_5H_4-COOC_5H_4N$) **L**^{2} gives **5** and **6** in good yield (Scheme 1). The products are obtained by precipitation as air-stable orange or red powders.

Compounds **1**−**5** are soluble in halogenated solvents and polar organic solvents such as tetrahydrofuran, methanol, or dimethyl sulfoxide and also in water. In contrast, **6** dissolves only in methanol and dimethyl sulfoxide. All complexes were characterized by IR, ^{1}H and ^{13}C{^{1}H} NMR spectroscopy, and mass spectrometry (see Experimental Section).

In addition, the structure of **4** has been confirmed by a single-crystal X-ray analysis and is shown in Figure 2; selected bond parameters are given in the caption. The ruthenium center in **4** possesses a pseudo-octahedral geometry, and the metrical parameters around the metallic core compare well with those of the three-legged piano-stool complex [Ru(η^6-C_6Me_6)(NC_5H_5)Cl_2] and other related imidazole species.[31] The pyridyl substituent is rotated out of the ester plane by 69.7°. The ferrocene moiety is in the eclipsed conformation and shows no interaction with neighboring molecules of **4**. Thus, the cavities between the complexes contain chloroform molecules.

Table 1. Electrochemical Data for **L**^{1} and Complexes **1**−**4**[a]

compound	Fe^{II}/Fe^{III} $E^{\circ\prime}$/V ΔE_p[mV]	Ru^{II}/Ru^{III} E_{pa}/V
L^1	0.33 (80)	n.a.
1	0.34 (80)	E_{pa} 1.00
2	0.34 (80)	E_{pa} 0.97
3	0.34 (80)	E_{pa} 0.91
4	0.34 (80)	$E^{\circ\prime}$ (ΔE_p) 0.65 (75)

[a] Potentials are given relative to ferrocene/ferrocenium reference (see Experimental Section for details). Peak potentials for irreversible processes were obtained at scan rate of 100 mV s^{-1}. $E^{\circ\prime} = 1/2(E_{pa} + E_{pc})$, $\Delta E_p = E_{pa} - E_{pc}$.

Electrochemical Study. The electrochemical behavior of the ferrocenecarboxylic esters **L**^{1} and **L**^{2} and ruthenium(η^6-arene) complexes **1**−**5** has been studied by cyclic voltammetry at a stationary platinum disc and by voltammetry at a rotating platinum disc electrode (Pt-RDE) using ca. 5×10^{-4} M dichloromethane solutions containing 0.1 M tetrabutylammonium hexafluorophosphate as the supporting electrolyte. The data for **L**^{1} and its ruthenium complexes are summarized in Table 1, while the redox response of **L**^{2} and complex **5** is discussed in the text.[32]

Ligand **L**^{1} represents the simplest compound in the series and undergoes one-electron reversible oxidation within the whole potential range followed (from ca. −2.2 to +1.4 V vs ferrocene/ferrocenium reference). Characteristics: $i_{pa} \propto \nu^{1/2}$, $i_{pa}/i_{pc} \approx 1$, and $i_{lim} \propto \omega^{1/2}$. The oxidation is attributable to the ferrocene/ferrocenium redox couple and, in accordance with the presence of the electron-withdrawing ester group

(23) Dale, L. D.; Tocher, J. H.; Dyson, T. M.; Edwards, D. I.; Tocher, D. A. *Anti-Cancer Drug Des.* **1992**, *7*, 3−14.
(24) Allardyce, C. S.; Dyson, P. J.; Ellis, D. J.; Heath, S. L. *Chem. Commun.* **2001**, 1396−1397. (b) Scolaro, C.; Bergamo, A.; Brescacin, L.; Delfino, R.; Cocchietto, M.; Laurenczy, G.; Geldbach, T. J.; Sava, G.; Dyson, P. J. *J. Med. Chem.* **2005**, *48*, 4161−4171.
(25) Morris, R. E.; Aird, R. E.; Murdoch, P. D. S.; Chen, H.; Cummings, J.; Hughes, N. D.; Parsons, S.; Parkin, A.; Boyd, G.; Jodrell, D. I.; Sadler, P. J. *J. Med. Chem.* **2001**, *44*, 3616−3621.
(26) Therrien, B.; Ang, W. H.; Chérioux, F.; Vieille-Petit, L.; Juillerat-Jeanneret, L.; Süss-Fink, G.; Dyson, P. J. *J. Cluster Sci.* **2007**, *18*, 741−752.
(27) Allardyce, C. S.; Dyson, P. J. *J. Cluster Sci.* **2001**, *12*, 563−569.
(28) (a) Bennett, M. A.; Smith, A. K. *J. Chem. Soc., Dalton Trans.* **1974**, 233−241. (b) Bennett, M. A.; Huang, T.-N.; Matheson, T. W.; Smith, A. K. *Inorg. Synth.* **1982**, *21*, 74−76.
(29) Auzias, M.; Therrien, B.; Labat, G.; Stoeckli-Evans, H.; Süss-Fink, G. *Inorg. Chim. Acta* **2006**, *359*, 1012−1017.
(30) Auzias, M.; Therrien, B.; Süss-Fink, G. *Inorg. Chem. Commun.* **2007**, *10*, 1239−1243.
(31) Steedman, A. J.; Burrell, A. K. *Acta Crystallogr.* **1997**, *C53*, 864−866. (b) Vock, C. A.; Scolaro, C.; Phillips, A. D.; Scopelitti, R.; Sava, G.; Dyson, P. J. *J. Med. Chem.* **2006**, *49*, 5552−5561.
(32) Definitions: E_{pa} and E_{pc} are anodic and cathodic peak potentials, respectively. Similarly, i_{pa} and i_{pc} denote the anodic and cathodic peak currents in cyclic voltammetry. i_{lim} is the limiting current in voltammetry at Pt-RDE, ν the scan rate, and ω the rotation frequency of the disc electrode.

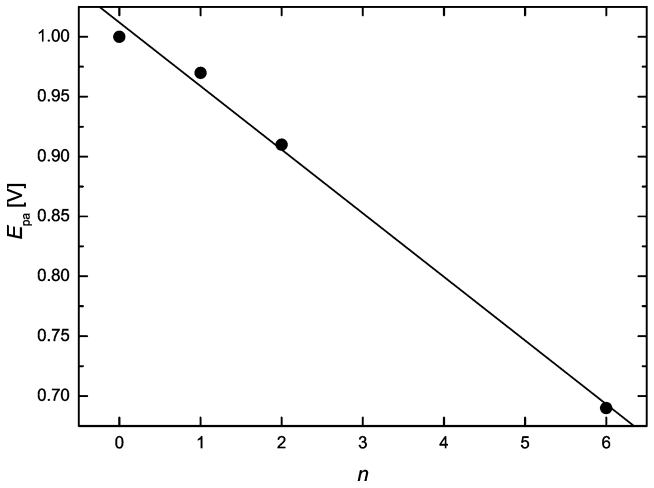

Figure 3. Correlation between the number of alkyl substituents on the arene ring (n) and the anodic peak potentials for the Ru-centered oxidation in the series of complexes **1** ($n = 0$), **2** ($n = 1$), **3** ($n = 2$), and **4** ($n = 6$). Parameters of the linear fit: $E_{pa} = 1.012(9) - 0.053(3)n$ ($R = 0.997$).

at the ferrocene unit, occurs at a more positive value, by 0.33 V, than the oxidation of ferrocene itself.

Coordination of the pyridine nitrogen atom in $\mathbf{L^1}$ to a Ru(η^6-arene)Cl_2 unit has only a negligible effect on the redox potential of the ferrocene/ferrocenium couple (see Table 1). This rules out any significant electronic coupling between the ferrocene unit and the peripheral pyridyl group or indicates an efficient compensation of the influence of the coordinated metal by π-back-donation. However, the presence of the Ru(II) center in **1**−**4** is reflected by an additional wave due to the Ru^{II}/Ru^{III} couple.

The redox response of the Ru(η^6-arene) unit is strongly influenced by the arene ligand, particularly by the number of attached alkyl groups. As expected, increasing the number of electron-donating alkyl groups at the arene ring makes the $Ru^{II} \rightarrow Ru^{III}$ oxidation more facile. A linear correlation between the anodic peak potential and the number of alkyl groups is observed, see Figure 3, which indicates that the contributions from the individual alkyl groups are essentially additive.

Moreover, the increased bulkiness of the arene ring positively influences the reversibility of the Ru^{II}/Ru^{III} redox process and also hinders sorption of the compounds at the electrode surface. For the η^6-benzene complex **1**, the Ru-centered oxidation is irreversible up to 500 mV s^{-1} and associated with sorption processes that influence the preceding (Fe^{II}/Fe^{III}) redox step. When scanned with the switching potential set just after the first oxidation wave, the ferrocene oxidation is observed with full reversibility (Figure 4a). Raising the switching potential beyond the Ru-based oxidation probably triggers deposition of the electrogenerated species at the electrode surface, and the reduction of the ferrocenium species during back scanning is observed, convoluted with electrode desorption and hence with $i_{pc} > i_{pa}$ (Figure 4b).

The presence of the alkyl substituents on the arene ring apparently makes the electrode adsorption difficult. Consequently, the Ru-centered oxidations in complexes **2** and **3** are observed with partial reversibility at higher scan rates

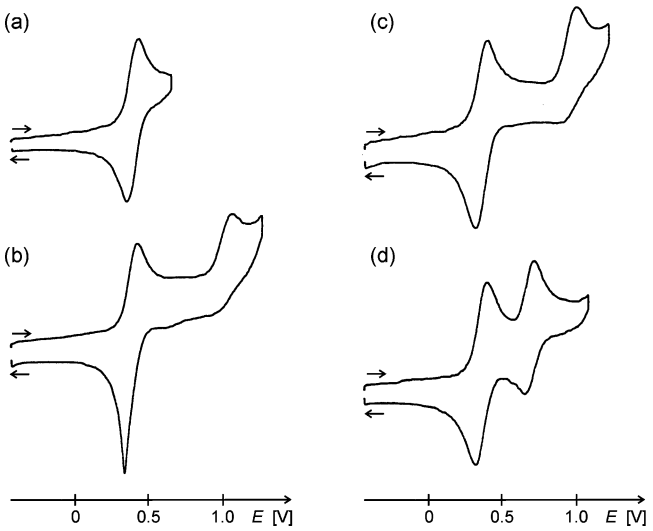

Figure 4. Cyclic voltammograms of **1** (a,b), **2** (c), and **4** (d) (common details: 100 mV s^{-1} scan rate, platinum disc electrode, dichloromethane solutions).

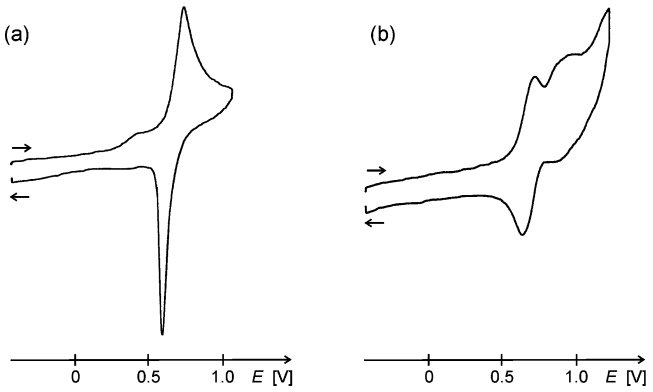

Figure 5. Cyclic voltammograms of $\mathbf{L^2}$ (a) and **5** (b) recorded in dichloromethane solutions at platinum disc electrode and with 100 mV s^{-1} scan rate.

($E_{pc} \approx 0.83$ V for **3** at 500 mV s^{-1}) and, due to a higher electron-donating ability of the arene ring, shifted to lower potentials (see Figure 4c). Finally, total ring substitution such that in **4** makes the Ru^{II}/Ru^{III} redox process fully reversible even at 50 mV s^{-1} (Figure 4d).

Similarly to $\mathbf{L^1}$, the diester $\mathbf{L^2}$ becomes oxidized in a single one-electron step at $E_{pa} = 0.60$ V vs ferrocene/ferrocenium. However, the oxidation is associated with a strong electrode adsorption (Figure 5a). The adsorption is reflected also in voltammograms recorded at Pt-RDE that show only 'humps', the peak currents of which drop upon decreasing the scan rate due to extensive electrode coverage. In contrast, the ferrocene/ferrocenium oxidation in complex **5** is affected much less, showing signs of electrochemical reversibility ($E^{\circ\prime} = 0.64$ V, $\Delta E_p = 80$ mV; Figure 5b). The following oxidative steps centered at the ruthenium atoms give rise to poorly resolved broad waves. The related compound **6** could not be studied due to its poor solubility in dichloromethane.

Cell Growth Inhibition on A2780 and A2780cisR Cell Lines. The ability of the complexes to inhibit cancer cell growth was evaluated using the MTT assay which measures mitochondrial dehydrogenase activity as an indication of cell viability (see Experimental Section). The test was carried

Table 2. IC_{50} Values of Complexes **1**−**6** on A2780 and A2780cisR Human Ovarian Cancer Cells after Drug Exposure

complexes	ligand	IC_{50} (μM) with standard deviations	
		A2780	A2780cisR
$[Ru(\eta^6\text{-}C_6H_6)Cl_2(NC_5H_4OOC\text{-}C_5H_4FeC_5H_5)]$, **1**	$\mathbf{L}^1$	34.3 (4.1)	39.3 (10.2)
$[Ru(\eta^6\text{-}C_6H_5Me)Cl_2(NC_5H_4OOC\text{-}C_5H_4FeC_5H_5)]$, **2**	$\mathbf{L}^1$	49.5 (5.0)	57.0 (4.4)
$[Ru(\eta^6\text{-}p\text{-}^iPrC_6H_4Me)Cl_2(NC_5H_4OOC-C_5H_4FeC_5H_5)]$, **3**	$\mathbf{L}^1$	44.5 (4.7)	43.4 (3.4)
$[Ru(\eta^6\text{-}C_6Me_6)Cl_2(NC_5H_4OOC-C_5H_4FeC_5H_5)]$, **4**	$\mathbf{L}^1$	38.1 (4.4)	44.1 (5.1)
$[Ru(\eta^6\text{-}p\text{-}^iPrC_6H_4Me)Cl_2]_2(NC_5H_4OOC-C_5H_4FeC_5H_4-COOC_5H_4N)$, **5**	$\mathbf{L}^2$	19.3 (3.5)	17.0 (2.6)
$[Ru(\eta^6\text{-}C_6Me_6)Cl_2]_2(NC_5H_4OOC-C_5H_4FeC_5H_4-COOC_5H_4N)$, **6**	$\mathbf{L}^2$	14.8 (2.4)	17.7 (6.1)
cisplatin *cis*-$[Pt(NH_3)_2Cl_2]$		1.6	8.6

out using **1**−**6** on human ovarian carcinoma cell lines A2780 and its cisplatin-resistant strain A2780cisR. The effects of compounds **1**−**6** on the viability of these cells were evaluated after an exposure period of 72 h. The IC_{50} values, corresponding to inhibition of cancer cell growth at the 50% level, are listed in Table 2.

For the mono-ruthenium arene complexes **1**−**4** their cytotoxicity is not directly correlated with the number of alkyl substituents on the coordinated arene ligands (and hence with their redox properties) since the activity decreased in the sequence benzene (**1**) > hexamethylbenzene (**4**) > *p*-cymene (**3**) > toluene (**2**). In fact, this sequence differs from that observed for related ruthenium(II)−arene complexes of formula $[Ru(\eta^6\text{-}C_6Me_6)Cl_2(pta)]$ in which the toluene derivative is the most cytotoxic.[24]

Interestingly, diruthenium arene complexes **5** and **6** were approximately twice as active as their monoruthenium analogues **3** and **4**, respectively, suggesting that the active part of these complexes is due to the ruthenium−arene motif. This behavior is in contrast to that observed for ruthenium−arene complexes connected via an alkyl chain which did not show increased cytotoxic effects relative to their mononuclear counterparts.[33] However, it cannot be ruled out that the quite different redox potential of the ferrocene unit in **5** and **6** relative to **1**−**4** is responsible, at least in part, for the increased cytotoxicity. Although, the IC_{50} values are higher than cisplatin, they are comparatively low for ruthenium compounds which tend to be less active in vitro, although they are often highly active in vivo. Significantly, the complexes were equally potent toward both the A2780 and cisplatin-resistant A2780cisR human ovarian carcinoma cell lines. It is known that cisplatin exerts its cytotoxic effect through DNA-binding interactions leading to apoptotic cell death.[34] The data presented here suggests that the mechanism of action of **1**−**6** is different from that of cisplatin since resistance in the A2780cisR cells has been attributed to increased DNA repair.[35]

Experimental Section

General. All reagents were purchased either from Aldrich, Fluka, or Acros and used without further purification. All manipulations were carried out under nitrogen atmosphere. All solvents were distilled over appropriate drying agents and N_2-saturated prior to use. NMR spectra were measured on a Bruker 400 spectrometer at 20 °C. IR spectra were recorded on a Perkin-Elmer 1720X FT-IR spectrometer (4000−400 cm^{-1}). Electrospray mass spectra were obtained in positive-ion mode on a LCQ Finnigan mass spectrometer. 1-Ferrocenecarboxylic acid pyridin-4-yl ester[29] $\mathbf{L^1}$ and 1,1′-ferrocene dicarboxylic acid pyridin-4-yl ester[30] $\mathbf{L^2}$, $[RuCl_2(arene)]_2$[28] were prepared as previously described.

Synthesis of $[Ru(\eta^6\text{-arene})Cl_2(NC_5H_4OOC-C_5H_4FeC_5H_5)]$. To a solution of $[Ru(\eta^6\text{-arene})Cl_2]_2$ in dichloromethane (20 mL), 1-ferrocenecarboxylic acid pyridin-4-yl ester ($\mathbf{L^1}$) (2.4 equiv) was added. The mixture was stirred at room temperature for 24 h. Then the product was isolated by precipitation with diethyl ether and dried in vacuo to afford a red-orange crystalline powder. Alternatively, the reaction has also been performed in refluxing toluene (20 mL) for 24 h with the same results. All compounds have been isolated in pure form according to the NMR spectra; however, none of the compounds gave satisfactory microanalytical results for unknown reasons.

$[Ru(\eta^6\text{-}C_6H_6)Cl_2(NC_5H_4OOC-C_5H_4FeC_5H_5)]$, 1. Yield: 85%. ^1H NMR (400 MHz, CD_2Cl_2): δ = 4.30 (s, 5H, C_5H_5), 4.60 (t, 2H, J = 2 Hz, C_5H_4), 4.96 (t, 2H, J = 2 Hz, C_5H_4), 5.66 (s, 6H, C_6H_6), 7.32 (d, 2H, J = 7 Hz, NC_5H_4), 9.06 (d, 2H, J = 7 Hz, NC_5H_4). ^{13}C NMR (100 MHz, CD_2Cl_2): δ = 68.27 (C_{ipso} of Fc), 70.20, 70.79, 72.89 (*C*H of Fc), 84.42 (C_6H_6), 117.59 (NCH-*C*H), 156.41 (N*C*H−CH), 159.38 (*C*-OOC), 168.75 (*C*OO). IR (CaF_2, CH_2Cl_2): $\nu_{(OCO)}$ 1740 (m) cm^{-1}. ESI-MS ($(CH_3)_2CO$): m/z = 521.95 $[M - Cl]^+$.

$[Ru(\eta^6\text{-}C_6H_5Me)Cl_2(NC_5H_4OOC-C_5H_4FeC_5H_5)]$, 2. Yield: 81%. ^1H NMR (400 MHz, CD_2Cl_2): δ = 2.19 (s, 3H, C*H*$_3$), 4.34 (s, 5H, C_5H_5), 4.63 (t, 2H, J = 2 Hz, C_5H_4), 4.99 (t, 2H, J = 2 Hz, C_5H_4), 5.32−5.36 (m, 2H, C_6H_5), 5.56−5.69 (m, 3H, C_6H_5), 7.35 (d, 2H, J = 7 Hz, NC_5H_4), 9.07 (d, 2H, J = 7 Hz, NC_5H_4). ^{13}C NMR (100 MHz, CD_2Cl_2): δ = 19.09 (*C*H$_3$), 68.69 (C_{ipso} of Fc), 70.60, 71.18, 73.27 (*C*H of Fc), 80.07, 81.64, 87.38 (*C*H), 100.56 (*C*-CH$_3$), 117.95 (NCH−*C*H), 156.71 (N*C*H−CH), 159.73 (*C*−OOC), 169.15 (*C*OO). IR (CaF_2, CH_2Cl_2): $\nu_{(OCO)}$ 1740 (m) cm^{-1}. ESI-MS ($CHCl_3$/CH_3OH/$(CH_3)_2CO$): m/z = 571.94 $[M + H]^+$, 535.96 $[M - Cl]^+$.

$[Ru(\eta^6\text{-}p\text{-}^iPrC_6H_4Me)Cl_2(NC_5H_4OOC-C_5H_4FeC_5H_5)]$, 3. Yield: 90%. ^1H NMR (400 MHz, CD_2Cl_2): δ = 1.35 (d, 6H, J = 6.92 Hz, CH(C*H*$_3$)$_2$), 2.12 (s, 3H, C*H*$_3$), 3.00 (sept, 1H, J = 6.92 Hz, C*H*(CH$_3$)$_2$), 4.33 (s, 5H, C_5H_5), 4.63 (t, 2H, J = 2 Hz, C_5H_4), 4.99 (t, 2H, J = 2 Hz, C_5H_4), 5.27 (d, 2H, J = 6 Hz, C_6H_4), 5.48 (d, 2H, J = 6 Hz, C_6H_4), 7.33 (d, 2H, J = 6.8 Hz, NC_5H_4), 9.03 (d, 2H, J = 6.8 Hz, NC_5H_4). ^{13}C NMR (100 MHz, CD_2Cl_2): δ = 18.43 (*C*H$_3$), 22.41 (CH(*C*H$_3$)$_2$), 31.08 (*C*H(CH$_3$)$_2$), 68.74 (C_{ipso} of Fc), 70.60, 71.18, 73.28 (*C*H of Fc), 83.17, 82.46 (*C*H), 97.43 (*C*−CH$_3$), 103.63 (*C*−CH(CH$_3$)$_2$), 117.92 (NCH−*C*H), 156.54 (N*C*H−CH), 159.65 (*C*−OOC), 169.12 (*C*OO). IR (CaF_2, CH_2Cl_2): $\nu_{(OCO)}$ 1740 (m) cm^{-1}. ESI-MS ($CHCl_3$/CH_3OH): m/z = 613.99 $[M + H]^+$, 578.94 $[M - Cl]^+$.

$[Ru(\eta^6\text{-}C_6Me_6)Cl_2(NC_5H_4OOC-C_5H_4FeC_5H_5)]$, 4. Yield: 38%. ^1H NMR (400 MHz, $CDCl_3$): δ = 2.04 (s, 18H, C*H*$_3$), 4.30 (s,

(33) Chen, H.; Parkinson, J. A.; Nováková, O.; Bella, J.; Wang, F.; Dawson, A.; Gould, R.; Parsons, S.; Brabec, V.; Sadler, P. J. *Proc. Natl. Acad. Sci. U.S.A.* **2003**, *100*, 14623−14628.
(34) Reedijk, J.; Lohman, P. H. M. *Pharm. World Sci.* **1985**, *7*, 173−180.
(35) Masuda, H.; Ozols, R. F.; Lai, G.-M.; Fojo, A.; Rothenberg, M.; Hamilton, T. C. *Cancer Res.* **1988**, *48*, 5713−5716.

5H, C_5H_5), 4.59 (t, 2H, J = 2 Hz, C_5H_4), 4.97 (t, 2H, J = 2 Hz, C_5H_4), 7.27 (dd, 2H, J = 2 Hz, J = 6 Hz, NC_5H_4), 8.85 (dd, 2H, J = 2 Hz, J = 6 Hz, NC_5H_4). ^{13}C NMR (100 MHz, $CDCl_3$): δ = 15.89, 16.31 (CH_3), 68.65 (C_{ipso} of Fc), 70.56, 71.20, 73.18 (*C*H of Fc), 90.00, 91.65 ($C-CH_3$), 117.94 (NCH−*C*H), 156.33 (N*C*H−CH), 159.40 (*C*−OOC), 169.37 (*C*OO). IR (CaF_2, CH_2Cl_2): $\nu_{(OCO)}$ 1740 (m) cm^{-1}. ESI-MS ($CHCl_3$/CH_3OH): m/z = 606.00 [M − Cl]$^+$.

Synthesis of [Ru(η^6-arene)Cl$_2$]$_2$(1,1′-(NC$_5$H$_4$−OOC)$_2$−C$_5$H$_4$FeC$_5$H$_4$). To a solution of [Ru(η^6-arene)Cl_2]$_2$ in dichloromethane (20 mL), 1,1′-ferrocene dicarboxylic acid pyridin-4-yl ester (**L^2**) (1 equiv) was added. The mixture was stirred at room temperature for 24 h (for the hexamethylbenzene derivative precipitation occurred after some hours). Then the product was isolated by precipitation with diethyl ether and dried in vacuum to afford an orange crystalline powder.

[Ru(η^6-*p*-^{i}PrC$_6$H$_4$Me)Cl$_2$]$_2$(1,1′-(NC$_5$H$_4$−OOC)$_2$−C$_5$H$_4$FeC$_5$H$_4$), 5. Yield: 74%. ^{1}H NMR (400 MHz, CD_2Cl_2): δ = 1.34 (d, 12H, J = 6.92 Hz, $CH(CH_3)_2$), 2.09 (s, 6H, CH_3), 3.00 (sept, 2H, J = 6.92 Hz, $CH(CH_3)_2$), 4.73 (s, 4H, C_5H_4), 5.07 (s, 4H, C_5H_4), 5.30 (d, 4H, J = 5.7 Hz, C_6H_4), 5.50 (d, 4H, J = 5.7 Hz, C_6H_4), 7.31 (d, 4H, J = 6.4 Hz, NC_5H_4), 9.02 (d, 4H, J = 6.4 Hz, NC_5H_4). ^{13}C NMR (100 MHz, CD_2Cl_2): δ = 18.46 (CH_3), 22.42 ($CH(CH_3)_2$), 31.11 ($CH(CH_3)_2$), 68.74 (C_{ipso} of Fc), 73.12, 74.52 (*C*H of Fc), 83.31, 82.42 (*C*H), 97.54 ($C-CH_3$), 103.53 (*C*−$CH(CH_3)_2$), 118.06 (NCH−*C*H), 156.68 (N*C*H−CH), 159.28 (*C*−OOC), 167.64 (*C*OO). IR (CaF_2, CH_2Cl_2): $\nu_{(OCO)}$ 1745 (m) cm^{-1}. ESI-MS ($CHCl_3$/CH_3OH): m/z = 1004.98 [M − Cl]$^+$, 735.01 [M − ($C_{10}H_{14}RuCl_2$)]$^+$, 699.03 [M − ($C_{10}H_{14}RuCl_2$) − Cl]$^+$, 576.93 [M − ($C_{10}H_{14}RuCl_2$) − Cl − (NC_5H_4OOC)]$^+$.

[Ru(η^6-C$_6$Me$_6$)Cl$_2$]$_2$(1,1′-(NC$_5$H$_4$−OOC)$_2$−C$_5$H$_4$FeC$_5$H$_4$), 6. Yield: 92%. ^{1}H NMR (400 MHz, CD_3OD): δ = 2.09 (s, 36H, CH_3), 4.80 (t, 4H, J = 2 Hz, C_5H_4), 4.28 (t, 4H, J = 2 Hz, C_5H_4), 7.37 (dd, 4H, J = 1.2 Hz, J = 6 Hz, NC_5H_4), 8.10 (dd, 4H, J = 1.2 Hz, J = 6 Hz, NC_5H_4). IR (KBr): $\nu_{(OCO)}$ 1745 (m) cm^{-1}. ESI-MS ($CHCl_3$/CH_3OH): m/z = 1063.05 [M − Cl]$^+$, 727.06 [M − ($C_{12}H_{18}RuCl_2$) − Cl]$^+$, 633.00 [M − ($C_{12}H_{18}RuCl_2$) − Cl − (NC_5H_4O)]$^+$.

Crystallographic Analysis. Crystal data for **4**·($CHCl_3$)$_2$: $C_{30}H_{33}Cl_8FeN_2Ru$, Triclinic space group $P-1$ (No. 2), cell parameters a = 10.4816(5) Å, b = 12.8132(7) Å, c = 13.7867(7) Å, α = 98.901(4)°, β = 107.379(4)°, γ = 97.329(4)°, V = 1715.88(15) Å^3, T = 173(2) K, Z = 2, D_c = 1.703 g cm^{-3}, F(000) 884, λ (Mo Kα) = 0.71073 Å, 9258 reflections measured, 8060 unique (R_{int} = 0.0414) which were used in all calculations. The structure was solved by direct methods (SHELXS-97)[36] and refined (SHELXL-97)[37] by full-matrix least-squares methods on F^2 with 394 parameters. R_1 = 0.0303 ($I > 2\sigma(I)$) and wR_2 = 0.0789, GOF = 1.046; max/min residual density 2.036/−1.321 eÅ^{-3}. The H atoms were included in calculated positions and treated as riding atoms using the SHELXL default parameters. Figure 2 was drawn with ORTEP,[38] and the structural data were deposited at The Cambridge Crystallographic Data Centre: CCDC 657155.

Electrochemistry. Electrochemical measurements were carried out on a multipurpose polarograph PA3 interfaced to a Model 4103 XY recorded (Laboratorní př ístroje, Prague) at room temperature using a standard three-electrode cell with rotating platinum disc electrode (RDE; 1 mm diameter) as the working electrode, a platinum wire as the auxiliary electrode, and a saturated calomel electrode (SCE) reference electrode. The reference electrode was separated from the analyzed solution by a salt bridge filled with 0.1 M $Bu_4N[PF_6]$ in dichloromethane. The samples were dissolved in dichloromethane (Merck, p.a.) to give a concentration of 5 × 10^{-4} M of the analyte and 0.1 M $Bu_4N[PF_6]$ (Fluka, purissimum for electrochemistry). The solutions were purged with argon prior to measurement and then kept under an argon blanket. Cyclic voltammograms were recorded at a stationary platinum disc electrode (scan rates 50−500 mV s^{-1}), while the voltammograms were obtained at RDE (1000−2500 rpm, scan rate 20 mV s^{-1}). Redox potentials are given relative to the ferrocene/ferrocenium reference.

Cell Culture and Inhibition of Cell Growth. Human A2780 and A2780cisR ovarian carcinoma cell lines were obtained from the European Centre of Cell Cultures (ECACC, Salisbury, U.K.) and maintained in culture as described by the provider. The cells were routinely grown in RPMI 1640 medium containing 10% fetal calf serum (FCS) and antibiotics at 37 °C and 6% CO_2. For evaluation of growth inhibition tests, the cells were seeded in 96-well plates (Costar, Integra Biosciences, Cambridge, MA) and grown for 24 h in complete medium. Complexes **1**−**6** and rHSA solutions were diluted directly in culture medium to the required concentration and added to the cell culture for 72 h incubation. The MTT test was performed for the last 2 h without changing the culture medium and performed in triplicate. Briefly, following drug exposure, MTT (Sigma) was added to the cells at a final concentration of 0.2 mg/mL and incubated for 2 h; then the culture medium was aspirated and the violet formazan precipitate dissolved in 0.1 N HCl in 2-propanol. The optical density was quantified at 540 nm using a multiwell plate reader (iEMS Reader MF, Labsystems), and the percentage of surviving cells was calculated from the ratio of absorbance of treated to untreated cells. The IC_{50} values for the inhibition of cell growth were determined by fitting the plot of the percentage of surviving cells against the drug concentration using a sigmoidal function (Origin v7.5).

Acknowledgment. Financial support of this work by the Swiss National Science Foundation and a generous loan of ruthenium(III) chloride hydrate from the Johnson Matthey Research Centre are gratefully acknowledged. This work is also a part of the long-term research plan of Faculty of Science, Charles University, supported by the Ministry of Education of the Czech Republic (project no. MSM 0021620857).

Supporting Information Available: Crystallographic data for **4**·($CHCl_3$)$_2$ in CIF format and concentration−cytotoxicity response curves. This material is available free of charge via the Internet at http://pubs.acs.org.

IC7018742

(36) Sheldrick, G. M. *SHELXS-97*, *Program for Crystal Structure Solution*; University of Göttingen: Göttingen, Germany, 1997.
(37) Sheldrick, G. M. *SHELXL-97*, *Program for Crystal Structure Refinement*; University of Göttingen: Göttingen, Germany, 1997.
(38) Farrugia, L. J. *J. Appl. Crystallogr.* **1997**, *30*, 565.